

Asynchronous Federated Reinforcement Learning with Policy Gradient Updates: Algorithm Design and Convergence Analysis

Guangchen Lan, Dong-Jun Han, Abolfazl Hashemi, Vaneet Aggarwal, Christopher G. Brinton
Purdue University, West Lafayette, IN, USA
{lan44, han762, abolfazl, vaneet, cgb}@purdue.edu

ABSTRACT

To improve the efficiency of reinforcement learning, we propose a novel asynchronous federated reinforcement learning framework termed AFedPG, which constructs a global model through collaboration among N agents using policy gradient (PG) updates. To handle the challenge of lagged policies in asynchronous settings, we design delay-adaptive lookahead and normalized update techniques that can effectively handle the heterogeneous arrival times of policy gradients. We analyze the theoretical global convergence bound of AFedPG, and characterize the advantage of the proposed algorithm in terms of both the sample complexity and time complexity. Specifically, our AFedPG method achieves $O(\frac{\epsilon^{-2.5}}{N})$ sample complexity at each agent on average. Compared to the single agent setting with $O(\epsilon^{-2.5})$ sample complexity, it enjoys a linear speedup with respect to the number of agents. Moreover, compared to synchronous FedPG, AFedPG improves the time complexity from $O(\frac{t_{\max}}{N})$ to $O(\frac{1}{\sum_{i=1}^N \frac{1}{t_i}})$, where t_i denotes the time consumption in each iteration at the agent i , and t_{\max} is the largest one. The latter complexity $O(\frac{1}{\sum_{i=1}^N \frac{1}{t_i}})$ is always smaller than the former one, and this improvement becomes significant in large-scale federated settings with heterogeneous computing powers ($t_{\max} \gg t_{\min}$). Finally, we empirically verify the improved performances of AFedPG in three MuJoCo environments with varying numbers of agents. We also demonstrate the improvements with different computing heterogeneity.¹

CCS CONCEPTS

• **Computing methodologies** → **Machine learning; Artificial intelligence**; • **Computer systems organization** → *Distributed architectures*; • **Networks** → *Network services*.

KEYWORDS

Reinforcement Learning, Policy Gradient, Federated Learning, Asynchronous, Optimization

¹The Technical Report with proof details is available on arXiv [23].

Permission to make digital or hard copies of all or part of this work for personal or classroom use is granted without fee provided that copies are not made or distributed for profit or commercial advantage and that copies bear this notice and the full citation on the first page. Copyrights for components of this work owned by others than the author(s) must be honored. Abstracting with credit is permitted. To copy otherwise, or republish, to post on servers or to redistribute to lists, requires prior specific permission and/or a fee. Request permissions from permissions@acm.org.

MobiHoc '24, October 14–17, 2024, Athens, Greece

© 2024 Copyright held by the owner/author(s). Publication rights licensed to ACM.
ACM ISBN 978-1-4503-XXXX-X/18/06...\$15.00
<https://doi.org/XXXXXXXX.XXXXXXX>

ACM Reference Format:

Guangchen Lan, Dong-Jun Han, Abolfazl Hashemi, Vaneet Aggarwal, Christopher G. Brinton, Purdue University, West Lafayette, IN, USA, {lan44, han762, abolfazl, vaneet, cgb}@purdue.edu . 2024. Asynchronous Federated Reinforcement Learning with Policy Gradient Updates: Algorithm Design and Convergence Analysis. In *Proceedings of International Symposium on Theory, Algorithmic Foundations, and Protocol Design for Mobile Networks and Mobile Computing (MobiHoc '24)*. ACM, New York, NY, USA, 13 pages. <https://doi.org/XXXXXXXX.XXXXXXX>

1 INTRODUCTION

Policy gradient (PG) methods, also known as REINFORCE [49], are widely used to solve reinforcement learning (RL) problems across a range of applications, with recent notable examples including reinforcement learning from human feedback (RLHF) in Google's Gemma [44], OpenAI's InstructGPT [37], and ChatGPT (GPT-4 [36]). It has also garnered significant attention in networking and communication communities for solving network optimization problems, e.g., scheduling [48] and queueing [15], and solving wireless communication problems, e.g., wireless video streaming [54], MAC design [32] and metaverse latency optimization [52].

Most practical RL applications are on large scales and rely on a huge amount of data samples for model training in an online behavior [26, 41], which is considered as the key bottleneck of RL [7, 22]. To reduce sample complexity while enabling training on massive data, a conventional approach involves transmitting locally collected samples from distributed agents to a central server [40]. The transmitted samples can then be used for policy learning on the server side. However, this may not be feasible in real-world mobile systems where the communication bandwidth is limited and a large training time is intolerable [14, 24, 35], such as wireless edge devices [12, 24], Internet of Things [9, 34], autonomous driving [20], and vehicle transportation [3, 11]. In RL, since new data is continuously generated based on the current policy, the samples collected at the agents need to be transmitted frequently to the server throughout the training process, resulting in a significant bottleneck with large delays. Furthermore, the sharing of individual data collected by agents may lead to privacy and legal issues [18, 33].

Federated learning (FL) [13, 28] offers a promising solution to the above challenges in a distributed setting. In FL, instead of directly transmitting the raw datasets to the central server, agents only communicate locally trained model parameters (or gradients) with the server. Although FL has been mostly studied for supervised learning problems, several recent works expanded the scope of FL to federated reinforcement learning (FedRL), where N agents collaboratively learn a global policy without sharing the trajectories they collected during agent-environment interaction [17, 19, 51]. FedRL has been studied in the tabular case [2, 17, 19], and for value-function based algorithms [46, 51], where a linear speedup has

Table 1: Performance improvements of our AFedPG over other policy gradient methods. We compare the complexity for global convergence in each agent.

	PG	FedPG	AFedPG (ours)
Sample Complexity	$\mathcal{O}(\epsilon^{-2.5})$	$\mathcal{O}(\frac{\epsilon^{-2.5}}{N})$	$\mathcal{O}(\frac{\epsilon^{-2.5}}{N})$
Global Time	-	$\mathcal{O}(\frac{t_{\max}}{N}\epsilon^{-2.5})$	$\mathcal{O}(\bar{t}\epsilon^{-2.5})$

been demonstrated. For policy-gradient based algorithms, namely FedPG, we note that linear speedup is easy to see as the trajectories collected by each agent could be parallelized [25]. However, policy-gradient based FedRL has not been well studied in terms of *global* (non-local) convergence and time complexity.

Despite all the aforementioned works in FedRL, they still face challenges in terms of time complexity, primarily due to their focus on synchronous model aggregation. In large-scale heterogeneous settings [4, 50], performing synchronous global updates has limitations, as the overall time consumption heavily depends on the slow agents, *i.e.*, stragglers [29]. In this paper, we aim to tackle this issue by strategically leveraging asynchronous federated learning (A-FL) in policy-based FedRL for the first time. A-FL [50] shows superiority compared to synchronous FL, and recent works [21, 29] further improve convergence performances with theoretical guarantees. However, compared to prior A-FL approaches focusing on supervised learning, integrating A-FL with policy-based FedRL introduces new challenges due to the presence of *lagged policies* in asynchronous settings. Unlike supervised FL where the datasets of the clients are fixed, in RL, agents collect new samples in each iteration based on the current policy. This dynamic nature of the data collection process makes both the problem itself and the theoretical analysis challenging. To the best of our knowledge, this problem setting and its challenges have been largely overlooked in existing research, despite the significance of employing FL in RL. The key question that this paper aims to address is:

Despite the inherent challenge of dealing with lagged policies among different agents, can we improve the efficiency of FedPG through asynchronous methods while ensuring theoretical convergence?

We answer this question in the affirmative by proposing AFedPG, an algorithm that asynchronously updates the global policy using policy gradients from federated agents. The key components of the proposed AFedPG include a delay-adaptive lookahead technique, which addresses the inconsistent arrival times of updates during the training process. The improvement of AFedPG over other approaches is summarized in Table 1. Here, the global time is measured by the number of global updates \times time complexity in each iteration. In terms of sample complexity, the federated learning technique brings a linear speedup with respect to the number of agents N . As for the global time, AFedPG improves from $\mathcal{O}(\frac{t_{\max}}{N}\epsilon^{-2.5})$ to $\mathcal{O}(\bar{t}\epsilon^{-2.5})$, where $\bar{t} := 1/\sum_{i=1}^N \frac{1}{t_i}$ is a harmonic average and always smaller than t_{\max}/N , and t_i denotes the time complexity in each iteration at agent i .

1.1 Summary of Contributions

Our main contributions can be summarized as follows:

- (1) **New methodology with a delay-adaptive technique:** We propose AFedPG, an asynchronous training method tailored to FedRL. To handle the delay issue in the asynchronous FedRL setting, we design a delay-adaptive lookahead technique. Specifically, in the k -th iteration of training, the agent collects samples according to the local model parameters $\tilde{\theta}_k \leftarrow \theta_k + \frac{1-\alpha_k-\delta_k}{\alpha_k-\delta_k}(\theta_k - \theta_{k-1})$, where δ_k is the delay. This updating technique cancels out the second-order correction terms and thus assists the convergence analysis.
- (2) **Convergence analysis:** This work gives the *global* convergence guarantees of the federated policy-based RL for the first time. We analytically characterize the convergence bound of AFedPG using the key lemmas, and show the impact of various parameters including delay and number of iterations in our analysis.
- (3) **Linear speedup in sample complexity:** As shown in Table 1, our federated method improves the sample complexity in each agent from $\mathcal{O}(\epsilon^{-2.5})$ (single agent PG) to $\mathcal{O}(\frac{\epsilon^{-2.5}}{N})$, where N is the number of federated agents. This represents the linear speedup with respect to the number of agents N .
- (4) **Time complexity improvement:** Our AFedPG also reduces the time complexity of synchronous FedPG from $\mathcal{O}(\frac{t_{\max}}{N})$ to $\mathcal{O}(\bar{t} := \frac{1}{\sum_{i=1}^N \frac{1}{t_i}})$. The latter is always smaller than the former. This gap is significant in large-scale federated settings with heterogeneous computing powers ($t_{\max} \gg t_{\min}$).
- (5) **Experiments under MuJoCo environment:** We empirically verify the improved performances of AFedPG in three different MuJoCo environments with varying numbers of agents. We also demonstrate the improvements with different computing heterogeneity.

To the best of our knowledge, this is the first work to successfully integrate policy-based reinforcement learning with asynchronous federated learning and analyze its behavior. This new setting necessitates us to deal with the lagged policies under a time-varying data scenario depending on the current policy.

Notation: We denote the Euclidean norm by $\|\cdot\|$, and the vector inner product by $\langle \cdot, \cdot \rangle$. For a vector $a \in \mathbb{R}^n$, we use a^\top to denote the transpose of a . A calligraphic font letter denotes a set, *e.g.*, \mathcal{C} , and $|\mathcal{C}|$ denotes its cardinality. We use $\mathcal{C} \setminus \{j\}$ to denote a set that contains all the elements in \mathcal{C} except for j .

The remainder of this paper is organized as follows. In the next subsection, we summarize the related works. In Section 2, we introduce our problem setting, including some backgrounds on reinforcement learning and policy gradients. In Section 3, we describe our proposed AFedPG method. In Section 4, we analyze the global convergence rate of AFedPG and discuss its time complexity compared to the synchronous setting. Section 5 presents the experimental results, and we conclude this paper in Section 6.

1.2 Related Work

In this subsection, we review previous works that are most relevant to the present work.

Policy gradient methods: For vanilla PG, the state-of-the-art result is presented in [55], achieving a sample complexity of $\tilde{\mathcal{O}}(\epsilon^{-4})$ for the local convergence. Several recent works have improved this

boundary with PG variants. In [16], a PG with momentum method is proposed with convergence rate $\mathcal{O}(\epsilon^{-3})$ for the local convergence. The authors of [6] further improve the convergence analysis of PG with momentum and achieve a global convergence with the rate $\mathcal{O}(\epsilon^{-3})$. In [10], a normalized PG technique is introduced and improves the global convergence rate to $\mathcal{O}(\epsilon^{-2.5})$. In [31], an acceleration-based natural policy gradient method is proposed with sample complexity $\mathcal{O}(\epsilon^{-2})$, but second-order matrices are computed in each iteration (with first-order information), which brings more computational cost. However, all previous works have focused on the single-agent scenario, and the federated PG has not been explored. Compared to these works, we focus on a practical federated PG setting with distributed agents to improve the efficiency of RL. Our scheme achieves linear speedup with respect to the number of agents, significantly reducing the sample complexity compared to the conventional PG approaches.

Asynchronous FL: In [50], the superiority of asynchronous federated learning (A-FL) has been empirically shown compared to synchronous FL in terms of convergence performances. In [4], the asynchronous analysis is extended to the vertical FL with a better convergence performance compared to the synchronous setting. In [8], a dropout regularization method is introduced to handle the heterogeneous problems in A-FL. About the same time, recent works [21, 29] further improve the convergence performance with theoretical guarantees, and show that A-FL always exceeds synchronous FL without any changes to the algorithm. We note that all previous A-FL works focus on supervised learning with fixed datasets on the client side. However, in RL, agents collect new samples that depend on the current policy (model parameters) in each iteration, which makes the problem fundamentally different and challenging. In this work, we address this challenge by developing an A-FL method highly tailored to policy gradient.

FedRL: For value-function based algorithms, [17] analyzes the convergence performances with environment heterogeneity. In [2], a local update method is used to reduce communication costs. [19] shows a linear speedup with respect to the number of agents. All of the above works are limited to tabular RL analysis. For actor-critic based method, [46] analyzes the convergence performances with linear function approximation. [30] builds a practical system to implement the neural network approximation. In [51], it adds KL divergence and experimentally validates the actor-critic based method with neural network approximation. For policy-based methods, in [25], it shows simplicity compared to the other RL methods, and a linear speedup has been demonstrated in the synchronous setting. However, with an online behavior, it is not practical to perform synchronous global updates with heterogeneous computing power, and the global time consumption heavily depends on the stragglers [29]. This motivates us to consider the asynchronous policy-based method for FedRL. We demonstrate both theoretically and empirically that our method further reduces the time complexity compared to the synchronous FedRL approach.

2 PROBLEM SETUP

Markov decision process: We consider the Markov decision process (MDP) as a tuple $(\mathcal{S}, \mathcal{A}, \mathcal{P}, \mathcal{R}, \gamma)$, where \mathcal{S} is the state space, \mathcal{A} is a finite action space, $\mathcal{P} : \mathcal{S} \times \mathcal{A} \times \mathcal{S} \rightarrow \mathbb{R}$ is a Markov kernel that

determines transition probabilities, $\mathcal{R} : \mathcal{S} \times \mathcal{A} \rightarrow \mathbb{R}$ is a reward function, and $\gamma \in (0, 1)$ is a discount factor. At each time step t , the agent executes an action $a_t \in \mathcal{A}$ from the current state $s_t \in \mathcal{S}$, following a stochastic policy π , i.e., $a_t \sim \pi(\cdot|s_t)$. The corresponding reward is defined as r_t . The state value function is defined as

$$V_\pi(s) = \mathbb{E}_{\substack{a_t \sim \pi(\cdot|s_t), \\ s_{t+1} \sim \mathcal{P}(\cdot|s_t, a_t)}} \left[\sum_{t=0}^{\infty} \gamma^t r(s_t, a_t) | s_0 = s \right]. \quad (1)$$

Similarly, the state-action value function (Q-function) is defined as

$$Q_\pi(s, a) = \mathbb{E}_{\substack{a_t \sim \pi(\cdot|s_t), \\ s_{t+1} \sim \mathcal{P}(\cdot|s_t, a_t)}} \left[\sum_{t=0}^{\infty} \gamma^t r(s_t, a_t) | s_0 = s, a_0 = a \right]. \quad (2)$$

An advantage function is then define as $A_\pi(s, a) = Q_\pi(s, a) - V_\pi(s)$. With continuous states, the policy is parameterized by $\theta \in \mathbb{R}^d$, and then the policy is referred as π_θ (Deep RL parameterizes π_θ by deep neural networks). A state-action visitation measure induced by π_θ is given as

$$v_{\pi_\theta}(s, a) = (1 - \gamma) \mathbb{E}_{s_0 \sim \rho} \left[\sum_{t=0}^{\infty} \gamma^t P(s_t = s, a_t = a | s_0, \pi_\theta) \right], \quad (3)$$

where the starting state s_0 is drawn from a distribution ρ . The goal of the agent is to maximize the expected discounted return defined as follows:

$$\max_{\theta} J(\theta) := \mathbb{E}_{s \sim \rho} [V_{\pi_\theta}(s)]. \quad (4)$$

The gradient of $J(\theta)$ can be written as [43]:

$$\nabla_{\theta} J(\theta) = \mathbb{E}_{\tau} \left[\sum_{t=0}^{\infty} \nabla_{\theta} \log \pi_{\theta}(a_t | s_t) \cdot A_{\pi_{\theta}}(s_t, a_t) \right], \quad (5)$$

where $\tau = (s_0, a_0, r_0, s_1, a_1, r_1 \dots)$ is a trajectory induced by policy π_θ . We omit the θ notation in the gradient operation and denote the policy gradient by g for short. Then, g is estimated by

$$g(\theta, \tau) = \sum_{t=0}^{\infty} \nabla \log \pi_{\theta}(a_t | s_t) \sum_{h=t}^{\infty} \gamma^h r(s_h, a_h). \quad (6)$$

Federated policy gradient: We aim to solve the above problem in an FL setting, where N agents collaboratively train a common policy π_θ . Specifically, each agent collects trajectories and corresponding reward $r(s_h, a_h)$ based on its local policy. Then, each agent i estimates $g(\theta_i, \tau)$ for training the model θ , and the updated models are aggregated at the server. Motivated by the limitations of synchronous model aggregation in terms of time complexity, in the next section, we present our AFedPG methodology that takes an asynchronous approach to solve (4) in a FL setting.

3 PROPOSED ASYNCHRONOUS FEDPG

The proposed algorithm consists of K global iterations, indexed by $k = 0, 1, \dots, K - 1$. We first introduce the definition of concurrency and delay in our asynchronous federated setting. We then present the proposed AFedPG methodology.

Definition 3.1. (Concurrency) We denote C_k as the set of active agents in the k -th global iteration, and define $\omega_k := |C_k|$ as the concurrency. We define the average and maximum concurrency as $\bar{\omega} := \frac{1}{K} \sum_{k=0}^{K-1} \omega_k$, and $\omega_{\max} := \max \omega_k$, respectively.

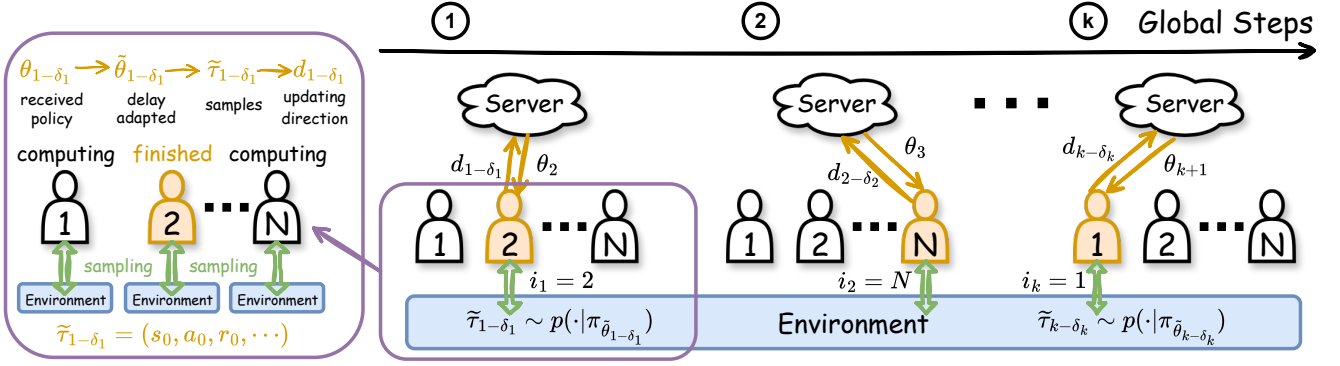


Figure 1: An illustration of the asynchronous federated policy gradient updates. Each agent has a local copy of the environment, and agents may collect data according to different local policies. At each iteration, the agent in the yellow color finishes the local process and then communicates with the server, while the other agents keep sampling and computing local gradients in parallel. In the k -th global iteration, $\delta_k \in \mathbb{N}$ is the delay, $\tilde{\tau}_{k-\delta_k}$ is the sample collected according to the policy $\pi_{\theta_{k-\delta_k}}$, and $d_{k-\delta_k}$ is the updating direction calculated from the sample $\tilde{\tau}_{k-\delta_k}$.

In each global iteration of AFedPG, the server applies only one gradient to update the model from the agent who has finished its local computation, while the other $N - 1$ agents keep computing local gradients (unapplied gradients) in parallel. In this asynchronous setting, the models used in each agent are outdated, as the server keeps updating the model. Thus, we introduce the notion of delay (or staleness) $\delta \in \mathbb{N}$, which measures the difference between the current global iteration and the past global iteration when the agent received the updated model from the server.

Definition 3.2. (Delay) In the k -th global iteration, we denote the delay of the applied gradient as $\delta_k \in \mathbb{N}$, and the delays of the unapplied gradients as $\{\delta_k^i\}_{i \in C_k \setminus \{j_k\}}$, where j_k denotes the agent that communicates with the server. δ_k^i is the difference between the k -th iteration and the iteration where the agent i started to compute the latest gradient. In the final K -th global iteration, we have K applied gradients $\{\delta_k\}_{k=0}^{K-1}$ and unapplied gradients $\{\delta_k^i\}_{i \in C_K \setminus \{j_K\}}$. The average and maximum delays can be expressed as

$$\bar{\delta} := \frac{1}{K-1+|C_K|} \left(\sum_{k=0}^{K-1} \delta_k + \sum_{i \in C_K \setminus \{j_K\}} \delta_k^i \right), \quad (7)$$

and $\delta_{\max} := \max(\max_k \delta_k, \max_{i \in C_K} \delta_k^i)$, respectively.

Asynchronous FedPG: Our goal is to train a global policy with parameters $\theta \in \mathbb{R}^d$ via FL across N distributed agents. As shown in Figure 1, during the training process, agent i collects trajectories in an online behavior, and computes gradients or updating directions using its *local trajectories* (also known as samples). Then, agent i transmits local gradients to the central server. In particular, in the k -th global iteration, the training of our AFedPG consists of the following three steps:

- **Local computation and uplink transmission:** Agent i receives the previous policy π_{θ_j} from the server in the j -th global iteration. Agent i collects its own local trajectory τ_j based on its current policy π_{θ_j} . Agent i then computes its

local updating direction $d_j \in \mathbb{R}^d$ based on the trajectory τ_j , and sends it back to the server.

- **Server-side model update:** The server starts to operate the k -th global iteration as soon as it receives d_j from agent i . Thus, denote $d_{k-\delta_k} = d_j$, where δ_k is the delay in the k -th global iteration. The server updates global policy parameters by $\theta \leftarrow \theta - \eta d_{k-\delta_k}$, where η is the learning rate.
- **Downlink transmission:** The server transmits the current global policy parameters $\theta \in \mathbb{R}^d$ back to agent i as soon as it finishes the global update.

The server side procedure of AFedPG is shown in Algorithm 1 and the process at the agent side is shown in Algorithm 2. In the k -th global iteration, the server operates one global update (Steps 4 and 5) as soon as it receives a direction $d_{k-\delta_k}$ from an agent with delay δ_k . After the global update, the server sends the updated model back to that agent. In Algorithm 2, after receiving the global model from the server, an agent first gets model parameters $\tilde{\theta}_k$ according to Step 2, and then collects samples based on the policy $\pi_{\tilde{\theta}_k}$ (Steps 3). At last, the agent computes the updating direction d_k , and sends it to the server as soon as it finishes the local process. Overall, all agents conduct local computation in parallel, but the global model is updated in an asynchronous manner as summarized in Figure 1.

Normalized update at the server: In Step 5 of Algorithm 1, to handle the updates with various delays, we use normalized gradients with controllable sizes. Specifically, the error term $\|e_k\|$ in Lemma 4.6 is related to $\|\nabla J(\tilde{\theta}_{k-\delta_k}) - \nabla J(\tilde{\theta}_k)\|$ and $\|\nabla J(\tilde{\theta}_{k-1}) - \nabla J(\tilde{\theta}_k)\|$. With the smoothness in Lemma 4.4, we are able to bound the error as $\|\theta_{k-1} - \theta_k\| = \eta_{k-1}$. The details of the boundaries are shown in (34).

Delay-adaptive lookahead at the agent: In Step 2 of Algorithm 2 (in blue), we design a delay-adaptive lookahead update technique, which operates as follows:

$$\theta_k = (1 - \alpha_{k-\delta_k})\theta_{k-1} + \alpha_{k-\delta_k}\tilde{\theta}_k. \quad (8)$$

Algorithm 1 AFedPG: Server.

Require: MDP $(\mathcal{S}, \mathcal{A}, \mathcal{P}, \mathcal{R}, \gamma)$; Number of iterations K ; Step size η_k, α_k ; Initial $\theta_0 \in \mathbb{R}^d$.

- 1: Broadcast θ_0 to N agents.
- 2: **for** $k = 0, \dots, K$ **do**
- 3: **▷ Server update**
- 4: Receive $d_{k-\delta_k}$ from the agent i_k .
- 5: $\theta_{k+1} \leftarrow \theta_k + \eta_k \frac{d_{k-\delta_k}}{\|d_{k-\delta_k}\|}$
- 6: **▷ Server broadcast**
- 7: Transmit θ_{k+1} back to the agent i_k .
- 8: **end for**

Ensure: θ^{K+1}

Algorithm 2 AFedPG: Agent i Update, $i = 1, \dots, N$.

Require: $\theta_k \in \mathbb{R}^d$

- 1: Receive θ_k from the server.
- 2: $\tilde{\theta}_k \leftarrow \theta_k + \frac{1-\alpha_k-\delta_k}{\alpha_k-\delta_k}(\theta_k - \theta_{k-1})$
- 3: $\tilde{\tau}_k \sim p(\cdot | \pi_{\tilde{\theta}_k})$
- 4: $d_k \leftarrow (1-\alpha_k)d_{k-1} + \alpha_k g(\tilde{\tau}_k, \tilde{\theta}_k)$
- 5: When finish computing, transmit d_k to the server.

Ensure: d_k

We note that (8) is not the conventional momentum method, because the orders are different. Here, $\tilde{\theta}_k$ "looks ahead" based on θ_{k-1} and θ_k , and the learning rate $\alpha_{k-\delta_k}$ depends on the delay δ_k .

In (8), the agent collects samples according to the current parameter $\tilde{\theta}_k$ in an online behavior, which only happens in the RL setting. This makes the problem fundamentally different from the conventional FL on supervised learning with a fixed dataset. This mechanism cancels out the second-order Hessian correction terms:

$$(1-\alpha_{k-\delta_k})\nabla^2 J(\theta_k)(\theta_{k-1}-\theta_k) + \alpha_{k-\delta_k}\nabla^2 J(\theta_k)(\tilde{\theta}_k-\theta_k) \rightarrow 0, \quad (9)$$

and thus assists the convergence analysis. The details are shown in Appendix A.2 in the Technical Report [23].

4 CONVERGENCE ANALYSIS

In this section, we derive the convergence rate of AFedPG with the following criteria for the global convergence.

Criteria: In this work, we focus on the global convergence, *i.e.*, finding the parameter θ *s.t.* $J^* - J(\theta) \leq \epsilon'$, where J^* is the optimal expected return.

4.1 Assumptions

In order to derive the global convergence rates, we make the following standard assumptions [1, 5, 27, 38, 53] on policy gradients, and rewards.

Assumption 4.1.

- (1) The score function is bounded as $\|\nabla \log \pi_\theta(a | s)\| \leq M_g$, for all $\theta \in \mathbb{R}^d, s \in \mathcal{S}$, and $a \in \mathcal{A}$.

- (2) The score function is M_h -Lipschitz continuous. In other words, $\forall \theta_i, \theta_j \in \mathbb{R}^d, s \in \mathcal{S}$, and $a \in \mathcal{A}$, we have

$$\left\| \nabla \log \pi_{\theta_i}(a | s) - \nabla \log \pi_{\theta_j}(a | s) \right\| \leq M_h \|\theta_i - \theta_j\|. \quad (10)$$

- (3) The reward function is bounded as $r(s, a) \in [0, R]$, for all $s \in \mathcal{S}$, and $a \in \mathcal{A}$.

These standard assumptions naturally state the reward, first-order and second-order derivatives of the score function are not infinite, and they hold with common practical parametrization methods, *e.g.*, softmax policies. With function approximation π_θ , the approximation error may not be 0 in practice. Thus, we follow previous works [1, 6, 16, 27] with an assumption on the expressivity of the policy parameterization class.

Assumption 4.2. (Function approximation) $\exists \epsilon_{bias} \geq 0$ *s.t.* for $\forall \theta \in \mathbb{R}^d$, the transfer error satisfies

$$\mathbb{E}[(A_{\pi_\theta}(s, a) - (1-\gamma)u^*(\theta)^\top \nabla \log \pi_\theta(a | s))^2] \leq \epsilon_{bias}, \quad (11)$$

where $u^*(\theta) := F_\rho(\theta)^\dagger \nabla J(\theta)$, and $F_\rho(\theta)^\dagger$ is the Moore-Penrose pseudo-inverse of the Fisher matrix F_ρ .

It means that the parameterized policy π_θ makes the advantage function $A_{\pi_\theta}(s, a)$ approximated by the score function $\nabla \log \pi_\theta(a | s)$ as the features. This assumption is widely used with Fisher-non-degenerate parameterization. ϵ_{bias} can be very small with rich neural network parameterization [47], and 0 with a soft-max parameterization [6].

4.2 Convergence Rates

Based on the above assumptions, the converges rate of AFedPG is given in Theorem 4.3.

Theorem 4.3. *Let Assumption 4.1 and 4.2 hold. With suitable learning rates η_k and α_k , after K global iterations, AFedPG satisfy*

$$J^* - \mathbb{E}[J(\theta_K)] \leq O(K^{-\frac{2}{5}} \cdot (1-\gamma)^{-3}) + \frac{\sqrt{\epsilon_{bias}}}{1-\gamma}, \quad (12)$$

where ϵ_{bias} is from (11). Thus, to satisfy $J^* - J(\theta_K) \leq \epsilon + \frac{\sqrt{\epsilon_{bias}}}{1-\gamma}$, we need $K = O(\frac{\epsilon^{-2.5}}{(1-\gamma)^{7.5}})$ iterations. As only one trajectory is required in each iteration, the number of trajectories is equal to K , *i.e.*, the sample complexity is $O(\frac{\epsilon^{-2.5}}{(1-\gamma)^{7.5}})$.

Comparison to the synchronous setting: Synchronous FedPG needs $O(\epsilon^{-2.5})$ trajectories in total, and each agent needs $O(\frac{\epsilon^{-2.5}}{N})$ trajectories. However, in synchronous FedGP the server has to wait for the slowest agent at each global step, which can still slow down the training process. Let t_i denote the time consumption for agent $i = 1, \dots, N$ at local steps with finite values. Then, the waiting time on the server for each step becomes $t_{\max} := \max t_i$ for FedPG. Our AFedPG approach keeps the same sample complexity as FedPG, but the server processes the global step as soon as it receives an update, speeding up training. Specifically, the average waiting time on the server is $\bar{t} := \frac{1}{\sum_{i=1}^N \frac{1}{t_i}} < \frac{t_{\max}}{N}$ at each step.

Thus, the asynchronous FedPG achieves better time complexity than the synchronous approach regardless of the delay pattern. The advantage is significant when $t_{\max} \gg t_{\min}$, which occurs in

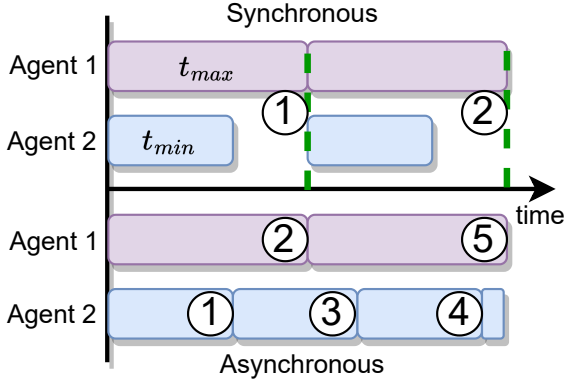


Figure 2: Comparison of time consumptions between synchronous and asynchronous approaches. The circled numbers denote the indices of global steps.

many practical settings with heterogeneous computation powers across different agents. We illustrate the advantage of AFedPG over synchronous FedPG in Figure 2. As the server only operates one simple summation, without loss of generality, the time consumption at the server-side is negligible.

4.3 Key Lemmas

We list some useful lemmas to construct the proof sketch of Theorem 4.3. The details of the proof can be found in Appendix A in the Technical Report [23].

Under Assumption 4.1 on score functions, the following lemma holds based on the results in [56].

Lemma 4.4. *The gradient of the expected return is L_g -continuous and L_h -smooth as follows*

$$\begin{aligned} \|\nabla J(\theta) - \nabla J(\theta')\| &\leq L_g \|\theta - \theta'\|, \\ \|\nabla^2 J(\theta) - \nabla^2 J(\theta')\| &\leq L_h \|\theta - \theta'\|, \end{aligned} \quad (13)$$

where $L_g := \frac{R(M_g^2 + M_h)}{(1-\gamma)^2}$ and $L_h := \frac{RM_g^3(1+\gamma)}{(1-\gamma)^3} + \frac{RM_g M_h}{(1-\gamma)^2} + \mathcal{O}((1-\gamma)^{-1})$.

Under Assumption 4.1 and 4.2, we utilize the result in [6] as the Lemma 4.5.

Lemma 4.5. *(Relaxed weak gradient domination) Under Assumptions 4.1 and 4.2, it holds that*

$$\|\nabla J(\theta)\| + \epsilon_g \geq \sqrt{2\mu}(J^* - J(\theta)), \quad (14)$$

where $\epsilon_g = \frac{\mu_F \sqrt{\epsilon_{\text{bias}}}}{M_g(1-\gamma)}$ and $\mu = \frac{\mu_F^2}{2M_g^2}$.

Based on Lemma 4.4, we derive our milestone, the ascent lemma with delayed updates, as follows:

Lemma 4.6. *(Ascent Lemma with Delay) Under Assumptions 4.1, it holds that*

$$-J(\theta_{k+1}) \leq -J(\theta_k) - \frac{1}{3}\eta_k \|\nabla J(\theta_k)\| + \frac{8}{3}\eta_k \|e_k\| + \frac{L_g}{2}\eta_k^2, \quad (15)$$

where $e_k := d_{k-\delta_k} - \nabla J(\theta_k)$.

This ascent lemma is specific to the asynchronous setting, which constructs the lower bound for the global increment, $J(\theta_{k+1}) - J(\theta_k)$, through the normalized policy gradients and our updating rules with delay δ_k .

PROOF. With the smoothness of the expected return $J(\theta)$ and the updating rule, we have

$$\begin{aligned} -J(\theta_{k+1}) &\leq -J(\theta_k) - \langle \nabla J(\theta_k), \theta_{k+1} - \theta_k \rangle + \frac{L_g}{2} \|\theta_{k+1} - \theta_k\|^2 \\ &= -J(\theta_k) - \eta_k \frac{\langle \nabla J(\theta_k), d_{k-\delta_k} \rangle}{\|d_{k-\delta_k}\|} + \frac{L_g}{2} \eta_k^2. \end{aligned} \quad (16)$$

If $\|e_k\| \leq \frac{1}{2} \|\nabla J(\theta_k)\|$, we have

$$\begin{aligned} -\frac{\langle \nabla J(\theta_k), d_{k-\delta_k} \rangle}{\|d_{k-\delta_k}\|} &= -\frac{\|\nabla J(\theta_k)\|^2 + \langle \nabla J(\theta_k), e_k \rangle}{\|d_{k-\delta_k}\|} \\ &\leq \frac{-\|\nabla J(\theta_k)\|^2 + \|\nabla J(\theta_k)\| \|e_k\|}{\|d_{k-\delta_k}\|} \\ &\leq \frac{-\|\nabla J(\theta_k)\|^2 + \frac{1}{2} \|\nabla J(\theta_k)\|^2}{\|\nabla J(\theta_k)\| + \|e_k\|} \leq -\frac{1}{3} \|\nabla J(\theta_k)\|. \end{aligned} \quad (17)$$

If $\|e_k\| \geq \frac{1}{2} \|\nabla J(\theta_k)\|$, we have

$$\begin{aligned} -\frac{\langle \nabla J(\theta_k), d_{k-\delta_k} \rangle}{\|d_{k-\delta_k}\|} &\leq \|\nabla J(\theta_k)\| \\ &= -\frac{1}{3} \|\nabla J(\theta_k)\| + \frac{4}{3} \|\nabla J(\theta_k)\| \leq -\frac{1}{3} \|\nabla J(\theta_k)\| + \frac{8}{3} \|e_k\|. \end{aligned} \quad (18)$$

Combine these two conditions, and plugging the result in (16), the lemma can be proved as

$$\begin{aligned} -J(\theta_{k+1}) &\leq -J(\theta_k) - \eta_k \frac{\langle \nabla J(\theta_k), d_{k-\delta_k} \rangle}{\|d_{k-\delta_k}\|} + \frac{L_g}{2} \eta_k^2 \\ &\leq -J(\theta_k) - \frac{1}{3} \eta_k \|\nabla J(\theta_k)\| + \frac{8}{3} \eta_k \|e_k\| + \frac{L_g}{2} \eta_k^2. \end{aligned} \quad (19)$$

□

Next, we construct the relationship between the average concurrency $\bar{\omega}$ and the average delay $\bar{\delta}$ in Lemma 4.7. This lemma gives the boundary (our result) of delays as a corollary of the result in [21].

Lemma 4.7. *The average delay $\bar{\delta}$ depends on the average concurrency $\bar{\omega}$ as*

$$\bar{\delta} = \frac{K+1}{K-1+|C_K|} \bar{\omega} \leq \bar{\omega} \leq N. \quad (20)$$

PROOF. Recall that $\{\delta_k^i\}_{i \in C_k \setminus \{j_k\}}$ is the set of delays at the k -th global steps. After one global step, the number of cumulative delays over all agents increases by the current concurrency. Thus, we have the following connection

$$\sum_{i=0}^k \delta_i + \sum_{i \in C_{k+1} \setminus \{j_{k+1}\}} \delta_{k+1}^i = \sum_{i=0}^{k-1} \delta_i + \sum_{i \in C_k \setminus \{j_k\}} \delta_k^i + \omega_{k+1}. \quad (21)$$

At the initial step, there is no delay. Therefore, we have $\delta_0^i = 0$ for all agents. Unrolling the above expression, at the K -th step, we

have

$$\sum_{i=0}^{K-1} \delta_i + \sum_{i \in C_K \setminus \{j_K\}} \delta_K^i = \sum_{i=0}^K \omega_{k+1} = (K+1)\bar{\omega}. \quad (22)$$

According to (7) and $|C_K| \geq 2$, we achieve

$$\bar{\delta} = \frac{K+1}{K-1+|C_K|} \bar{\omega} \leq \bar{\omega} \leq N. \quad (23)$$

In practice, we need to use all resources to speedup the training process, and thus, $\bar{\omega} = \omega_{\max} = N$. Since the maximum concurrency is equal to the number of agents N , we have the boundary of the average delay as $\bar{\delta} \leq \omega_{\max} \leq N$. \square

4.4 Proof sketch of Theorem 4.3

Here, we briefly give the main idea of our proof of Theorem 4.3. The complete details and the technical lemmas are provided in Appendix A in the Technical Report [23].

First, we prove the ascent lemma 4.6 based on Lemma 4.4 and the updating rule of AFedPG in Algorithm 1 and 2. We then plug it into (14) in Lemma 4.5 in the expectation form, and get the following inequality

$$J^* - \mathbb{E}[J(\theta_{k+1})] \leq (1 - \frac{\sqrt{2\mu}\eta_k}{3})(J^* - \mathbb{E}[J(\theta_k)]) + \frac{\eta_k}{3}\epsilon_g + \frac{8}{3}\eta_k\mathbb{E}[\|e_k\|] + \frac{L_g}{2}\eta_k^2. \quad (24)$$

Second, we bound the expected error term $\mathbb{E}[\|e_k\|]$ in the ascent lemma with delayed updates. Here we utilize the normalization and look-ahead sampling in Algorithm 1 and 2 to bound the error with an average delay term $\bar{\delta}$ from Lemma 4.7. With suitable learning rates as $\alpha_k = (\frac{1}{k+1})^{\frac{4}{5}}$ and $\eta_k = \eta_0 \frac{1}{k+1}$, the upper bound of $\mathbb{E}[\|e_k\|]$ is given as follows

$$\mathbb{E}[\|e_k\|] \leq \alpha_K \sigma_g + c_1 \sqrt{\alpha_K} \sigma_g + \frac{9}{4} c_2 L_h \frac{\eta_K^2}{\alpha_K^2} + 2c_3 L_g \frac{\eta_K^2}{\alpha_K} \bar{\delta}, \quad (25)$$

where c_1 , c_2 and c_3 are constants, and their values are given in Appendix A.2 in the Technical Report [23].

Third, unroll the recursion of (24), and then plug the upper bound result (25) into the unrolled form. We now have the following inequality

$$J^* - \mathbb{E}[J(\theta_K)] \leq \frac{\eta_0}{3} \epsilon_g + \frac{J^* - \mathbb{E}[J(\theta_0)]}{(K+1)^2} + c_3 \frac{16\eta_0^2}{3} \frac{L_g}{(K+1)^{\frac{7}{5}}} \bar{\delta} + \frac{\eta_0^2}{2} \frac{L_g}{K+1} + \frac{8\eta_0}{3} \frac{\sigma_g}{(K+1)^{\frac{4}{5}}} + c_1 \frac{8\eta_0}{3} \frac{\sigma_g}{(K+1)^{\frac{2}{5}}} + 6c_2 \eta_0^3 \frac{L_h}{(K+1)^{\frac{2}{5}}}. \quad (26)$$

With an initial learning rate as $\eta_0 = \frac{3\mu F}{M_g}$, we achieve the global convergence rate in Theorem 4.3.

5 EXPERIMENTS

5.1 Setup

Environment: To validate the effectiveness of our approach via experiments, we consider three popular MuJoCo environments (Swimmer-v4, Hopper-v4, and Humanoid-v4) [45] with the MIT

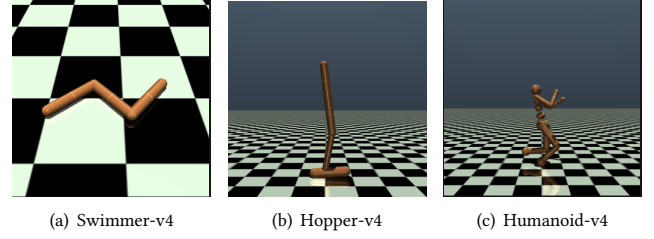


Figure 3: Visualization of the three MuJoCo tasks considered in this paper for experiments.

Table 2: Detailed descriptions of the three tasks in the MuJoCo environment.

MuJoCo Tasks	Agent Types	Action Space Dimension	State Space Dimension
Swimmer-v4	Three-link swimming robot	2	8
Hopper-v4	Two-dimensional one-legged robot	3	11
Humanoid-v4	Three-dimensional bipedal robot	17	376

Table 3: Hyperparameters of AFedPG and the MLP policy parameterization settings.

Hyperparameter	Setting		
Task	Swimmer-v4	Hopper-v4	Humanoid-v4
MLP	64 × 64	256 × 256	512 × 512 × 512
Activation function	ReLU	ReLU	ReLU
Output function	Tanh	Tanh	Tanh
Learning rate (α)	1×10^{-3}	1×10^{-3}	1×10^{-3}
Discount (γ)	0.99	0.99	0.99
Timesteps (T)	2048	1024	512
Iterations (K)	1×10^3	2×10^3	1.5×10^4
Learning rate (η)	3×10^{-4}	1×10^{-4}	1×10^{-5}

License. Both the state and action spaces are continuous. Environmental details are described in Table 2 and the MuJoCo tasks are visualized in Figure 3.

Measurement: All convergence performances are measured over 10 runs with random seeds from 0 to 9. The solid lines in our main experimental results are the averaged results, and the shadowed areas are confidence intervals with the confidence level 95%. The lines are smoothed for better visualization.

Implementation: Policies are parameterized by fully connected multi-layer perceptions (MLPs) with settings listed in Table 3. We follow the practical settings in stable-baselines3 [42] to update models with generalized advantage estimation (GAE) (0.95) [43] in our implementation. We use PyTorch [39] to implement deep

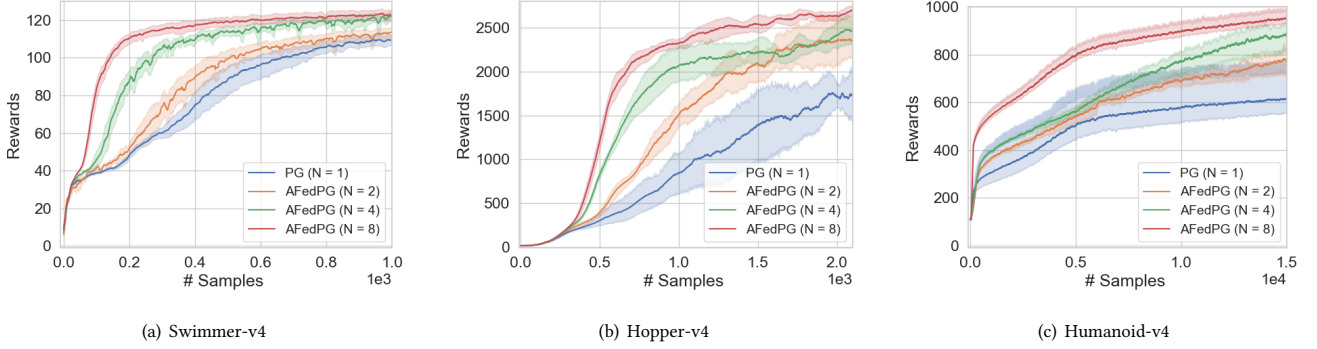


Figure 4: Reward performances of AFedPG ($N = 2, 4, 8$) and PG ($N = 1$) on various MoJuCo environments, where N is the number of federated agents. The solid lines are averaged results over 10 runs and the shadowed areas are confidence intervals with 95% confidence level.

neural networks (DNNs). All tasks are trained on NVIDIA A100 GPUs with 40 GB of memory.

Baselines: We first consider the conventional PG approach with $N = 1$, to see the effect of using multiple agents for improving sample complexity. We also consider the synchronous FedPG method as a baseline to observe the impact of asynchronous update for enhancing the time complexity. We note that only a few prior works have focused on the federated PG problem, and many existing works in federated supervised learning are not directly applicable to our federated RL setting.

Performance metrics: We consider the following metrics:

- (1) Rewards: the average trajectory rewards collected at each iteration;
- (2) Convergence: rewards versus iterations during the training process;
- (3) Time consumption: global time with certain numbers of collected samples.

5.2 Results

Speedup of sample complexity: First, to verify the improvement of sample complexity in the first row of Table 1, we evaluate the speedup effects of the number of federated agents N . In Figure 4, with different numbers of agents, we test the convergence performances of AFedPG ($N = 2, 4, 8$) and the single agent PG ($N = 1$). The x-axis is the number of samples collected by each agent on average, and the y-axis is the reward. In all three MuJoCo tasks, AFedPG beats the single-agent PG: AFedPG converges faster, has lower variances, and achieves higher final rewards when more agents are involved in collecting trajectories and estimating policy gradients. These results confirm the advantage of AFedPG in terms of sample complexity.

Improvement of global time complexity: Second, to verify the improvement of global time complexity in the second row of Table 1, we compared the time consumption in the asynchronous and synchronous settings. In Figure 5, we set $N = 4, 8$ and fix the number of samples collected by all agents. Here, t_{\max} is about 4 times more than t_{\min} . The numbers of total samples (trajectories)

are 8×10^3 , 16×10^3 , and 8×10^4 for the Swimmer-v4 task, Hopper-v4 task, and Humanoid-v4 task individually when $N = 8$. When $N = 4$, the numbers are halved. In all three environments, AFedPG has much lower time consumption compared to the synchronous FedPG, confirming the enhancement in terms of time complexity.

Effect of computation heterogeneity: At last, we study the effect of the computation heterogeneity among federated agents. The heterogeneity of computing powers is measured by the ratio $\frac{t_{\max}}{t_{\min}}$, and the effect is measured by the speedup, which is the global time of FedPG divided by that of AFedPG. Without loss of generality, we test the performances with one straggler here, which is one agent has t_{\max} time consumption, and all the other agents have t_{\min} time consumption. In Figure 6, the results show that the speedup increases in a nearly linear behavior as the heterogeneity ratio $\frac{t_{\max}}{t_{\min}}$ increases. On the other hand, the more agents that participate in the training process, the higher speedup they achieve. The overall results indicate that AFedPG has the potential to scale up to a very large mobile RL system, particularly in scenarios with extreme stragglers ($t_{\max} \gg t_{\min}$).

6 CONCLUSION

In this paper, we proposed AFedPG, a novel asynchronous federated reinforcement learning framework which updates the global model using policy gradients from multiple agents. To handle the challenge of lagged policies in the asynchronous setting, we designed a delay-adaptive lookahead technique and used normalized updates to integrate policy gradients. With the above methods, AFedPG achieves speedup for both sample complexity and time complexity. First, our AFedPG method achieves $O(\frac{\epsilon^{-2.5}}{N})$ sample complexity at each agent. Compared to the single agent setting (PG) with $O(\epsilon^{-2.5})$ sample complexity, it enjoys a linear speedup with respect to the number of agents N . Second, compared to synchronous FedPG, AFedPG improves the time consumption from $O(\frac{t_{\max}}{N})$ to $O(\frac{1}{\sum_{i=1}^N \frac{1}{t_i}})$, where t_i denotes the time consumption in each iteration at the agent i , and t_{\max} is the largest one. The latter complexity $O(\frac{1}{\sum_{i=1}^N \frac{1}{t_i}})$ is always smaller than the former one, and

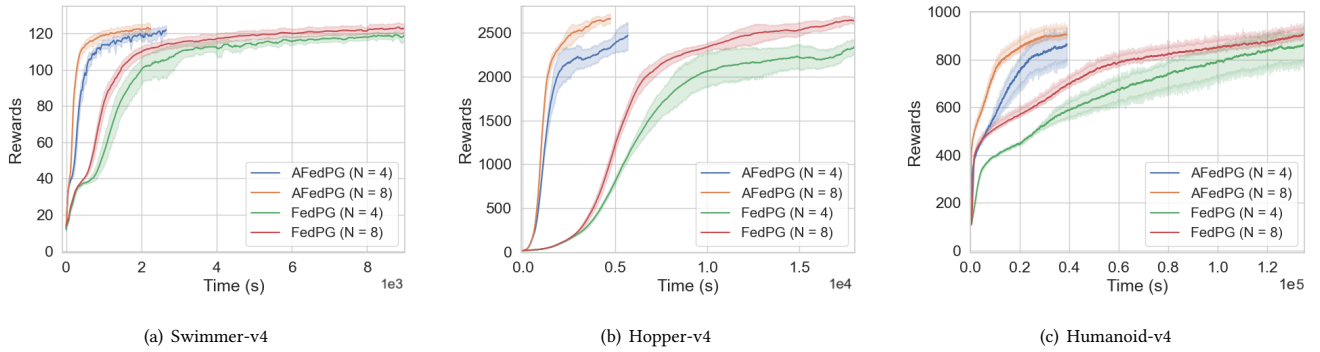


Figure 5: Global time of AFedPG and FedPG with certain numbers of collected samples on various MoJuCo environments, where N is the number of federated agents. The solid lines are averaged results over 10 runs and the shadowed areas are confidence intervals with 95% confidence level.

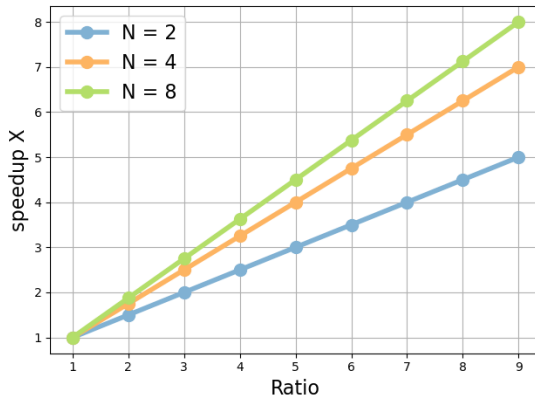


Figure 6: The time complexity speedup of AFedPG compared to FedPG. The x-axis is the heterogeneous ratio of computing power measured by $\frac{t_{\max}}{t_{\min}}$. The y-axis is the global time of FedPG divided by that of AFedPG.

this improvement can be significant in a large-scale federated setting with heterogeneous computing powers ($t_{\max} \gg t_{\min}$). Finally, we empirically verified the performances of AFedPG compared to PG and FedPG in three MuJoCo environments with different N . We also demonstrate the improvements with different computing heterogeneity. In summary, AFedPG achieves speedup in terms of both sample complexity and time complexity when it is scaled up to a large mobile RL system, especially with large computing power heterogeneity.

Investigating asynchronous FedRL with the second-order methods (e.g., natural policy gradients) and adversarial attacks are interesting directions for future research.

REFERENCES

- [1] Alekh Agarwal, Sham M. Kakade, Jason D. Lee, and Gaurav Mahajan. 2021. On the Theory of Policy Gradient Methods: Optimality, Approximation, and Distribution Shift. *Journal of Machine Learning Research* 22, 1 (2021), 4431–4506.
- [2] Mridul Agarwal, Bhargav Ganguly, and Vaneet Aggarwal. 2021. Communication Efficient Parallel Reinforcement Learning. In *Uncertainty in Artificial Intelligence (UAI 2021) (Proceedings of Machine Learning Research, Vol. 161)*. PMLR, 247–256.
- [3] Abubakr O. Al-Abbasi, Arnob Ghosh, and Vaneet Aggarwal. 2019. DeepPool: Distributed Model-free Algorithm for Ride-sharing Using Deep Reinforcement Learning. *IEEE Transactions on Intelligent Transportation Systems* 20, 12 (2019), 4714–4727.
- [4] Tianyi Chen, Xiao Jin, Yuejiao Sun, and Wotao Yin. 2020. VAFL: A Method of Vertical Asynchronous Federated Learning. *arXiv preprint arXiv:2007.06081* (2020).
- [5] Dongsheng Ding, Kaiqing Zhang, Tamer Basar, and Mihailo Jovanovic. 2020. Natural Policy Gradient Primal-Dual Method for Constrained Markov Decision Processes. In *Advances in Neural Information Processing Systems (NeurIPS 2020)*, Vol. 33. Curran Associates, Inc., 8378–8390.
- [6] Yuhao Ding, Junzi Zhang, and Javad Lavaei. 2022. On the Global Optimum Convergence of Momentum-based Policy Gradient. In *Proceedings of The 25th International Conference on Artificial Intelligence and Statistics (AISTAT 2022) (Proceedings of Machine Learning Research, Vol. 151)*. PMLR, 1910–1934.
- [7] Gabriel Dulac-Arnold, Nir Levine, Daniel J Mankowitz, Jerry Li, Cosmin Paduraru, Sven Gowal, and Todd Hester. 2021. Challenges of Real-world Reinforcement Learning: Definitions, Benchmarks and Analysis. *Machine Learning* 110, 9 (2021), 2419–2468.
- [8] Chen Dun, Mirian Hipolito, Chris Jermaine, Dimitrios Dimitriadis, and Anastasios Kyriklidis. 2023. Efficient and Light-Weight Federated Learning via Asynchronous Distributed Dropout. In *Proceedings of The 26th International Conference on Artificial Intelligence and Statistics (AISTAT 2023) (Proceedings of Machine Learning Research, Vol. 206)*. PMLR, Palau de Congressos, Valencia, Spain, 6630–6660.
- [9] Wenzhi Fang, Dong-Jun Han, and Christopher G. Brinton. 2023. Submodel Partitioning in Hierarchical Federated Learning: Algorithm Design and Convergence Analysis. *arXiv preprint arXiv:2310.17890* (2023).
- [10] Ilyas Fatkhullin, Anas Barakat, Anastasia Kireeva, and Niao He. 2023. Stochastic Policy Gradient Methods: Improved Sample Complexity for Fisher-nondegenerate Policies. In *International Conference on Machine Learning (ICML 2023) (Proceedings of Machine Learning Research, Vol. 202)*. PMLR, Honolulu, HI, USA, 9827–9869.
- [11] Marina Haliem, Ganapathy Mani, Vaneet Aggarwal, and Bharat Bhargava. 2021. A Distributed Model-free Ride-sharing Approach for Joint Matching, Pricing, and Dispatching Using Deep Reinforcement Learning. *IEEE Transactions on Intelligent Transportation Systems* 22, 12 (2021), 7931–7942.
- [12] Dong-Jun Han, Do-Yeon Kim, Minseok Choi, David Nickel, Jaekyun Moon, Mung Chiang, and Christopher G. Brinton. 2023. Federated Split Learning With Joint Personalization-Generalization for Inference-Stage Optimization in Wireless Edge Networks. *IEEE Transactions on Mobile Computing* (2023).
- [13] Seyyedali Hosseinalipour, Christopher G. Brinton, Vaneet Aggarwal, Huaiyu Dai, and Mung Chiang. 2020. From Federated to Fog Learning: Distributed Machine Learning over Heterogeneous Wireless Networks. *IEEE Communications Magazine* 58, 12 (2020), 41–47.
- [14] Pihe Hu, Yu Chen, Ling Pan, Zhixuan Fang, Fu Xiao, and Longbo Huang. 2024. Multi-User Delay-Constrained Scheduling with Deep Recurrent Reinforcement Learning. *IEEE/ACM Transactions on Networking* (2024).
- [15] Pihe Hu, Ling Pan, Yu Chen, Zhixuan Fang, and Longbo Huang. 2022. Effective Multi-user Delay-constrained Scheduling with Deep Recurrent Reinforcement Learning. In *Proceedings of the Twenty-Third International Symposium on Theory, Algorithmic Foundations, and Protocol Design for Mobile Networks and Mobile*

- Computing (MobiHoc 2022)*. Association for Computing Machinery, Seoul, South Korea, 1–10.
- [16] Feihu Huang, Shangqian Gao, Jian Pei, and Heng Huang. 2020. Momentum-based Policy Gradient Methods. In *International conference on machine learning (ICML 2020) (Proceedings of Machine Learning Research, Vol. 119)*. PMLR, 4422–4433.
 - [17] Hao Jin, Yang Peng, Wenhao Yang, Shusen Wang, and Zhihua Zhang. 2022. Federated Reinforcement Learning with Environment Heterogeneity. In *International Conference on Artificial Intelligence and Statistics (AISTAT 2022) (Proceedings of Machine Learning Research, Vol. 151)*. PMLR, 18–37.
 - [18] Peter Kairouz, H. Brendan McMahan, Brendan Avent, Aurélien Bellet, Mehdi Bennis, Arjun Nitin Bhagoji, Kallista Bonawitz, Zachary Charles, Graham Cormode, Rachel Cummings, et al. 2021. Advances and Open Problems in Federated Learning. *Foundations and trends® in machine learning* 14, 1–2 (2021), 1–210.
 - [19] Sajad Khodadadian, Pranay Sharma, Gauri Joshi, and Siva Theja Maguluri. 2022. Federated Reinforcement Learning: Linear Speedup under Markovian Sampling. In *International Conference on Machine Learning (ICML 2022)*, Vol. 162. PMLR, Baltimore, MD, USA, 10997–11057.
 - [20] B. Ravi Kiran, Ibrahim Sobh, Victor Talpaert, Patrick Mannion, Ahmad A. Al Sallab, Senthil Yogamani, and Patrick Pérez. 2022. Deep Reinforcement Learning for Autonomous Driving: A Survey. *IEEE Transactions on Intelligent Transportation Systems* 23, 6 (2022), 4909–4926.
 - [21] Anastasiia Koloskova, Sebastian U. Stich, and Martin Jaggi. 2022. Sharper Convergence Guarantees for Asynchronous SGD for Distributed and Federated Learning. In *Advances in Neural Information Processing Systems (NeurIPS 2022)*, Vol. 35. PMLR, New Orleans, LA, USA, 17202–17215.
 - [22] Pawel Ladosz, Lilian Weng, Minwoo Kim, and Hyondong Oh. 2022. Exploration in Deep Reinforcement Learning: A Survey. *Information Fusion* 85 (2022), 1–22.
 - [23] Guangchen Lan, Dong-Jun Han, Abolfazl Hashemi, Vaneet Aggarwal, and Christopher G. Brinton. 2024. Asynchronous Federated Reinforcement Learning with Policy Gradient Updates: Algorithm Design and Convergence Analysis. *arXiv preprint arXiv:2404.08003* (2024).
 - [24] Guangchen Lan, Xiao-Yang Liu, Yijing Zhang, and Xiaodong Wang. 2023. Communication-efficient Federated Learning for Resource-constrained Edge Devices. *IEEE Transactions on Machine Learning in Communications and Networking* 1 (2023), 210–224.
 - [25] Guangchen Lan, Han Wang, James Anderson, Christopher Brinton, and Vaneet Aggarwal. 2023. Improved Communication Efficiency in Federated Natural Policy Gradient via ADMM-based Gradient Updates. In *Thirty-seventh Conference on Neural Information Processing Systems (NeurIPS 2023)*, Vol. 36. Curran Associates, Inc., New Orleans, LA, USA, 59873–59885.
 - [26] Xiao-Yang Liu, Zechu Li, Zhuoran Yang, Jiahao Zheng, Zhaoran Wang, Anwar Walid, Jian Guo, and Michael I Jordan. 2021. ElegantRL-Podracr: Scalable and Elastic Library for Cloud-Native Deep Reinforcement Learning. In *Advances in Neural Information Processing Systems Workshop on Deep Reinforcement Learning*.
 - [27] Yanli Liu, Kaiqing Zhang, Tamer Basar, and Wotao Yin. 2020. An Improved Analysis of (Variance-reduced) Policy Gradient and Natural Policy Gradient Methods. In *Advances in Neural Information Processing Systems (NeurIPS 2020)*, Vol. 33. Curran Associates, Inc., 7624–7636.
 - [28] Brendan McMahan, Eider Moore, Daniel Ramage, Seth Hampson, and Blaise Aguera y Arcas. 2017. Communication-efficient Learning of Deep Networks from Decentralized Data. In *International Conference on Artificial Intelligence and Statistics (AISTAT 2017) (Proceedings of Machine Learning Research, Vol. 54)*. PMLR, Ft. Lauderdale, FL, USA, 1273–1282.
 - [29] Konstantin Mishchenko, Francis Bach, Mathieu Even, and Blake E Woodworth. 2022. Asynchronous SGD Beats Minibatch SGD under Arbitrary Delays. In *Advances in Neural Information Processing Systems (NeurIPS 2022)*, Vol. 35. PMLR, New Orleans, LA, USA, 420–433.
 - [30] Volodymyr Mnih, Adria Puigdomenech Badia, Mehdi Mirza, Alex Graves, Timothy Lillicrap, Tim Harley, David Silver, and Koray Kavukcuoglu. 2016. Asynchronous Methods for Deep Reinforcement Learning. In *Proceedings of The 33rd International Conference on Machine Learning (ICML 2016) (Proceedings of Machine Learning Research, Vol. 48)*. PMLR, New York, NY, USA, 1928–1937.
 - [31] Washim Uddin Mondal and Vaneet Aggarwal. 2024. Improved Sample Complexity Analysis of Natural Policy Gradient Algorithm with General Parameterization for Infinite Horizon Discounted Reward Markov Decision Processes. *arXiv preprint arXiv:2310.11677* (2024).
 - [32] Sangwoo Moon, Sumyeong Ahn, Kyunghwan Son, Jinwoo Park, and Yung Yi. 2021. Neuro-DCF: Design of Wireless MAC via Multi-Agent Reinforcement Learning Approach. In *Proceedings of the Twenty-Second International Symposium on Theory, Algorithmic Foundations, and Protocol Design for Mobile Networks and Mobile Computing (MobiHoc 2021)*. Association for Computing Machinery, 141–150.
 - [33] Viraaji Mothukuri, Reza M. Parizi, Seyedamin Pouriyeh, Yan Huang, Ali Dehghantaha, and Gautam Srivastava. 2021. A Survey on Security and Privacy of Federated Learning. *Future Generation Computer Systems* 115 (2021), 619–640.
 - [34] Dinh C. Nguyen, Ming Ding, Pubudu N. Pathirana, Aruna Seneviratne, Jun Li, and H. Vincent Poor. 2021. Federated Learning for Internet of Things: A Comprehensive Survey. *IEEE Communications Surveys & Tutorials* 23, 3 (2021), 1622–1658.
 - [35] Solmaz Niknam, Harpreet S. Dhillon, and Jeffrey H. Reed. 2020. Federated Learning for Wireless Communications: Motivation, Opportunities, and Challenges. *IEEE Communications Magazine* 58, 6 (2020), 46–51.
 - [36] OpenAI. 2023. GPT-4 Technical Report. *arXiv preprint arXiv:2303.08774* (2023).
 - [37] Long Ouyang, Jeffrey Wu, Xu Jiang, Diogo Almeida, Carroll Wainwright, Pamela Mishkin, Chong Zhang, Sandhini Agarwal, Katarina Slama, Alex Gray, John Schulman, Jacob Hilton, Fraser Kelton, Luke Miller, Maddie Simens, Amanda Askell, Peter Welinder, Paul Christiano, Jan Leike, and Ryan Lowe. 2022. Training Language Models to Follow Instructions with Human Feedback. In *Advances in Neural Information Processing Systems (NeurIPS 2022)*, Vol. 35. Curran Associates, Inc., New Orleans, LA, USA, 27730–27744.
 - [38] Matteo Papini, Damiano Binaghi, Giuseppe Canonaco, Matteo Pirodda, and Marcello Restelli. 2018. Stochastic Variance-Reduced Policy Gradient. In *Proceedings of the 35th International Conference on Machine Learning (ICML 2018) (Proceedings of Machine Learning Research, Vol. 80)*. PMLR, Stockholm, Sweden, 4026–4035.
 - [39] Adam Paszke, Sam Gross, Francisco Massa, Adam Lerer, James Bradbury, Gregory Chanan, Trevor Killeen, Zeming Lin, Natalia Gimelshein, Luca Antiga, et al. 2019. PyTorch: An Imperative Style, High-performance Deep Learning Library. In *Advances in Neural Information Processing Systems (NeurIPS 2019)*, Vol. 32. Curran Associates, Inc., Vancouver, Canada.
 - [40] Joel B. Predd, Sanjeev B. Kulkarni, and H. Vincent Poor. 2006. Distributed Learning in Wireless Sensor Networks. *IEEE Signal Processing Magazine* 23, 4 (2006), 56–69.
 - [41] Foster Provost and Tom Fawcett. 2013. Data Science and Its Relationship to Big Data and Data-driven Decision Making. *Big Data* 1, 1 (2013), 51–59.
 - [42] Antonin Raffin, Ashley Hill, Adam Gleave, Anssi Kanervisto, Maximilian Ernestus, and Noah Dormann. 2021. Stable-Baselines3: Reliable Reinforcement Learning Implementations. *Journal of Machine Learning Research* 22, 268 (2021), 1–8.
 - [43] John Schulman, Philipp Moritz, Sergey Levine, Michael Jordan, and Pieter Abbeel. 2018. High-Dimensional Continuous Control Using Generalized Advantage Estimation. *arXiv preprint arXiv:1506.02438* (2018).
 - [44] Gemma Team and Google DeepMind. 2024. Gemma: Open Models Based on Gemini Research and Technology. *arXiv preprint arXiv:2403.08295* (2024).
 - [45] Emanuel Todorov, Tom Erez, and Yuval Tassa. 2012. MuJoCo: A Physics Engine for Model-based Control. In *IEEE/RSJ International Conference on Intelligent Robots and Systems (IROS 2012)*. IEEE, Vilamoura-Algarve, Portugal, 5026–5033.
 - [46] Han Wang, Aritra Mitra, Hamed Hassani, George J Pappas, and James Anderson. 2023. Federated Temporal Difference Learning with Linear Function Approximation under Environmental Heterogeneity. *arXiv preprint arXiv:2302.02212* (2023).
 - [47] Lingxiao Wang, Qi Cai, Zhuoran Yang, and Zhaoran Wang. 2020. Neural Policy Gradient Methods: Global Optimality and Rates of Convergence. In *International Conference on Learning Representations (ICLR 2020)*.
 - [48] Honghao Wei, Xin Liu, Weina Wang, and Lei Ying. 2023. Sample Efficient Reinforcement Learning in Mixed Systems through Augmented Samples and Its Applications to Queueing Networks. In *Thirty-seventh Conference on Neural Information Processing Systems (NeurIPS 2023)*, Vol. 36. Curran Associates, Inc., New Orleans, LA, USA, 2033–2055.
 - [49] Ronald J. Williams. 1992. Simple Statistical Gradient-following Algorithms for Connectionist Reinforcement Learning. *Machine learning* 8 (1992), 229–256.
 - [50] Cong Xie, Sanmi Koyejo, and Indranil Gupta. 2020. Asynchronous Federated Optimization. In *12th Annual Workshop on Optimization for Machine Learning (OPT 2020)*.
 - [51] Zhijie Xie and Shenghui Song. 2023. FedKL: Tackling Data Heterogeneity in Federated Reinforcement Learning by Penalizing KL Divergence. *IEEE Journal on Selected Areas in Communications* 41, 4 (2023), 1227–1242.
 - [52] Guojun Xiong, Xudong Qin, Bin Li, Rahul Singh, and Jian Li. 2022. Index-aware Reinforcement Learning for Adaptive Video Streaming at the Wireless Edge. In *Proceedings of the Twenty-Third International Symposium on Theory, Algorithmic Foundations, and Protocol Design for Mobile Networks and Mobile Computing (MobiHoc 2022)*. Association for Computing Machinery, Seoul, South Korea, 81–90.
 - [53] Pan Xu, Felicia Gao, and Quanquan Gu. 2020. Sample Efficient Policy Gradient Methods with Recursive Variance Reduction. In *International Conference on Learning Representations (ICLR 2020)*.
 - [54] Wenhan Yu, Terence Jie Chua, and Jun Zhao. 2023. Asynchronous Hybrid Reinforcement Learning for Latency and Reliability Optimization in the Metaverse Over Wireless Communications. *IEEE Journal on Selected Areas in Communications* 41, 7 (2023), 2138–2157.
 - [55] Rui Yuan, Robert M. Gower, and Alessandro Lazaric. 2022. A General Sample Complexity Analysis of Vanilla Policy Gradient. In *Proceedings of The 25th International Conference on Artificial Intelligence and Statistics (AISTAT 2022) (Proceedings of Machine Learning Research, Vol. 151)*. PMLR, 3332–3380.
 - [56] Kaiqing Zhang, Alec Koppel, Hao Zhu, and Tamer Basar. 2020. Global Convergence of Policy Gradient Methods to (Almost) Locally Optimal Policies. *SIAM Journal on Control and Optimization* 58, 6 (2020), 3586–3612.

A PROOFS

A.1 Technical Lemmas

Lemma A.1. For arbitrary n vectors $\{\mathbf{a}_i \in \mathbb{R}^d\}_{i=1}^n$, we have

$$\left\| \sum_{i=1}^n \mathbf{a}_i \right\|^2 \leq n \sum_{i=1}^n \|\mathbf{a}_i\|^2. \quad (27)$$

Lemma A.2. Let $\alpha_k = (\frac{c}{t+c})^p$. $\forall p \in [0, 1]$ and $c \geq 1$, we have

$$1 - \alpha_{k+1} \leq \frac{\alpha_{k+1}}{\alpha_k}. \quad (28)$$

PROOF.

$$\begin{aligned} 1 - \alpha_{k+1} &= 1 - \left(\frac{c}{t+1+c}\right)^p \\ &\leq 1 - \frac{1}{t+1+c} \\ &\leq \frac{\alpha_{k+1}}{\alpha_k}. \end{aligned} \quad (29)$$

Straightforwardly, we have

$$\prod_{i=k}^{K-1} (1 - \alpha_{i+1}) \leq \frac{\alpha_K}{\alpha_k}. \quad (30)$$

□

Lemma A.3. Let $\alpha_k = (\frac{1}{k+1})^p$ and $\eta_k = \eta_0 (\frac{1}{k+1})^q$. $\forall p \in [0, 1]$, $q \geq 0$ and $\eta_0 \geq 0$, we have

$$\sum_{k=0}^{K-1} \eta_k \prod_{i=k+1}^{K-1} (1 - \alpha_i) \leq c(p, q) \frac{\eta_K}{\alpha_K}, \quad (31)$$

where $c(p, q) := \frac{2^{q-p}}{1-p} a \exp((1-p)2^p a^{1-p})$ is a constant, and $a = \max\left(\left(\frac{q}{(1-p)2^p}\right)^{\frac{1}{1-p}}, \left(\frac{2(q-p)}{(1-p)^2}\right)^{\frac{1}{1-p}}\right)$.

A.2 Proof of Theorem 4.3

Denote $\xi_k := g(\tilde{\tau}_k, \tilde{\theta}_k) - \nabla J(\tilde{\theta}_k)$. First, according to the updating rules in Algo. 1 and Algo. 2, we expand the error term in Lemma 4.6 as follows

$$\begin{aligned} e_k &= (1 - \alpha_{k-\delta_k})d_{\delta_{k-1}} + (1 - \alpha_{k-\delta_k})(\nabla J(\theta_{k-1}) - \nabla J(\theta_k)) + \alpha_{k-\delta_k}(g(\tilde{\tau}_{k-\delta_k}, \tilde{\theta}_{k-\delta_k}) - \nabla J(\theta_k)) \\ &= \alpha_{k-\delta_k}\xi_{k-\delta_k} + (1 - \alpha_{k-\delta_k})e_{k-1} + (1 - \alpha_{k-\delta_k})(\nabla J(\theta_{k-1}) - \nabla J(\theta_k)) + \alpha_{k-\delta_k}(\nabla J(\tilde{\theta}_{k-\delta_k}) - \nabla J(\theta_k)) \\ &= \alpha_{k-\delta_k}\xi_{k-\delta_k} + (1 - \alpha_{k-\delta_k})e_{k-1} + (1 - \alpha_{k-\delta_k})(\nabla J(\theta_{k-1}) - \nabla J(\theta_k)) \\ &\quad + \alpha_{k-\delta_k}(\nabla J(\tilde{\theta}_{k-\delta_k}) - \nabla J(\tilde{\theta}_k)) + \alpha_{k-\delta_k}(\nabla J(\tilde{\theta}_k) - \nabla J(\theta_k)) \\ &= \alpha_{k-\delta_k}\xi_{k-\delta_k} + (1 - \alpha_{k-\delta_k})e_{k-1} + (1 - \alpha_{k-\delta_k})(\nabla J(\theta_{k-1}) - \nabla J(\theta_k) + \nabla^2 J(\theta_k)(\theta_{k-1} - \theta_k)) \\ &\quad + \alpha_{k-\delta_k}(\nabla J(\tilde{\theta}_{k-\delta_k}) - \nabla J(\tilde{\theta}_k)) + \alpha_{k-\delta_k}(\nabla J(\tilde{\theta}_k) - \nabla J(\theta_k) + \nabla^2 J(\theta_k)(\theta_{k-1} - \theta_k)) \\ &\quad - (1 - \alpha_{k-\delta_k})\nabla^2 J(\theta_k)(\theta_{k-1} - \theta_k) - \alpha_{k-\delta_k}\nabla^2 J(\theta_k)(\tilde{\theta}_k - \theta_k) \\ &\stackrel{(8)}{=} \alpha_{k-\delta_k}\xi_{k-\delta_k} + (1 - \alpha_{k-\delta_k})e_{k-1} + (1 - \alpha_{k-\delta_k})(\nabla J(\theta_{k-1}) - \nabla J(\theta_k) + \nabla^2 J(\theta_k)(\theta_{k-1} - \theta_k)) \\ &\quad + \alpha_{k-\delta_k}(\nabla J(\tilde{\theta}_{k-\delta_k}) - \nabla J(\tilde{\theta}_k)) + \alpha_{k-\delta_k}(\nabla J(\tilde{\theta}_k) - \nabla J(\theta_k) + \nabla^2 J(\theta_k)(\theta_{k-1} - \theta_k)). \end{aligned} \quad (32)$$

Remark: The Hessian correction terms (in blue) are equal to 0 according to our updating rules (delay-adaptive lookahead update) in Step 2 of Algo. 2. We design this technique to cancel out the second-order terms, and thus achieve the desired convergence rate.

Next, we denote

$$\begin{aligned} A_k &:= \nabla J(\theta_{k-1}) - \nabla J(\theta_k) + \nabla^2 J(\theta_k)(\theta_{k-1} - \theta_k), \\ B_k &:= \nabla J(\tilde{\theta}_k) - \nabla J(\theta_k) + \nabla^2 J(\theta_k)(\theta_{k-1} - \theta_k), \\ C_k &:= \nabla J(\tilde{\theta}_{k-\delta_k}) - \nabla J(\tilde{\theta}_k). \end{aligned} \quad (33)$$

With the smoothness in Lemma 4.4 and the non-increasing learning rates, we have

$$\begin{aligned}
\|A_k\| &\leq L_h \|\theta_{k-1} - \theta_k\|^2 = L_h \eta_{k-1}^2, \\
\|B_k\| &\leq L_h \|\tilde{\theta}_k - \theta_k\|^2 = L_h \frac{(1 - \alpha_{k-\delta_k})^2}{\alpha_{k-\delta_k}^2} \eta_{k-1}^2, \\
\|C_k\| &\leq L_g \|\tilde{\theta}_{k-\delta_k} - \tilde{\theta}_k\| \\
&= L_g \left\| \sum_{i=k-\delta_k}^{k-1} \tilde{\theta}_{i+1} - \tilde{\theta}_i \right\| \\
&\leq L_g \sum_{i=k-\delta_k}^{k-1} \|\tilde{\theta}_{i+1} - \tilde{\theta}_i\| \\
&\leq L_g \sum_{i=k-\delta_k}^{k-1} \left(\frac{1}{\alpha_{i+1-\delta_{i+1}}} \eta_i + \frac{1 - \alpha_{i-\delta_i}}{\alpha_{i-\delta_i}} \eta_{i-1} \right) \\
&\leq L_g \sum_{i=k-\delta_k}^{k-1} \left(\frac{2}{\alpha_{k-1}} \eta_{k-\delta_k} \right) \\
&= \delta_k L_g \frac{2\eta_{k-\delta_k}}{\alpha_{k-1}}.
\end{aligned} \tag{34}$$

Denote $\beta_k := \prod_{i=k+1}^K (1 - \alpha_{i-\delta_i})$ with $\beta_K = 1$. Unrolling the recursion (32), we have

$$e_K = \beta_0 e_0 + \sum_{k=1}^K \alpha_{k-\delta_k} \beta_k \xi_{k-\delta_k} + \sum_{k=1}^K (1 - \alpha_{k-\delta_k}) \beta_k A_k + \sum_{k=1}^K \alpha_{k-\delta_k} \beta_k B_k. \tag{35}$$

Choose learning rates $\alpha_k = \left(\frac{1}{k+1}\right)^{\frac{4}{5}}$ and $\eta_k = \eta_0 \frac{1}{k+1}$, where η_0 is a constant and we will show the value later. Using Jensen's inequality and technical lemmas, we achieve the following bound

$$\begin{aligned}
\mathbb{E}[\|e_K\|] &\leq \beta_0 \mathbb{E}[\|e_0\|] + \mathbb{E} \left[\left\| \sum_{k=1}^K \alpha_{k-\delta_k} \beta_k \xi_{k-\delta_k} \right\|^2 \right]^{\frac{1}{2}} + \sum_{k=1}^K (1 - \alpha_{k-\delta_k}) \beta_k \mathbb{E}[\|A_k\|] \\
&\quad + \sum_{k=1}^K \alpha_{k-\delta_k} \beta_k (\mathbb{E}[\|B_k\|] + \mathbb{E}[\|C_k\|]) \\
&\stackrel{(34)}{\leq} \beta_0 \sigma_g + \left(\sum_{k=1}^K \alpha_{k-\delta_k}^2 \beta_k^2 \mathbb{E}[\|\xi_{k-\delta_k}\|^2] \right)^{\frac{1}{2}} + L_h \sum_{k=1}^K (1 - \alpha_{k-\delta_k}) \beta_k \eta_{k-1}^2 \\
&\quad + L_h \sum_{k=1}^K \beta_k \frac{(1 - \alpha_{k-\delta_k})^2}{\alpha_{k-\delta_k}} \eta_{k-1}^2 + 2L_g \sum_{k=1}^K \alpha_{k-\delta_k} \beta_k \delta_k \frac{\eta_{k-\delta_k}}{\alpha_{k-1}} \\
&\leq \beta_0 \sigma_g + \left(\sum_{k=1}^K \alpha_{k-\delta_k}^2 \beta_k^2 \right)^{\frac{1}{2}} \sigma_g + L_h \sum_{k=1}^K \frac{1}{\alpha_{k-\delta_k}} \beta_k \eta_{k-1}^2 + 2L_g \sum_{k=1}^K \alpha_{k-\delta_k} \beta_k \delta_k \frac{\eta_{k-\delta_k}}{\alpha_{k-1}} \\
&\stackrel{(30)}{\leq} \alpha_K \sigma_g + \left(\sum_{k=1}^K \alpha_{k-\delta_k}^2 \beta_k^2 \right)^{\frac{1}{2}} \sigma_g + \frac{9L_h}{4} \sum_{k=1}^K \frac{\eta_k^2}{\alpha_k} \beta_k + 2L_g \sum_{k=1}^K \alpha_{k-\delta_k} \beta_k \delta_k \frac{\eta_{k-\delta_k}}{\alpha_{k-1}} \\
&\stackrel{(31)}{\leq} \alpha_K \sigma_g + c_1 \sqrt{\alpha_K} \sigma_g + \frac{9}{4} c_2 L_h \frac{\eta_K^2}{\alpha_K^2} + 2c_3 L_g \frac{\eta_K^2}{\alpha_K} \bar{\delta},
\end{aligned} \tag{36}$$

where $c_1 := \sqrt{c(\frac{4}{5}, \frac{8}{5})}$, $c_2 := c(\frac{4}{5}, \frac{6}{5})$, $c_3 := c(\frac{4}{5}, 0)$ are constants, and the values of $c(\cdot, \cdot)$ are defined in Lemma A.3. After plugging the result into Lemma 4.6 and using Lemma 4.5, we achieve

$$\begin{aligned}
J^\star - \mathbb{E}[J(\theta_{k+1})] &\leq (1 - \frac{\sqrt{2\mu}\eta_k}{3})(J^\star - \mathbb{E}[J(\theta_k)]) + \frac{\eta_k}{3}\epsilon_g + \frac{8}{3}\eta_k\mathbb{E}[\|e_k\|] + \frac{L_g}{2}\eta_k^2 \\
&\stackrel{(36)}{\leq} (1 - \frac{\sqrt{2\mu}\eta_k}{3})(J^\star - \mathbb{E}[J(\theta_k)]) + \frac{\eta_k}{3}\epsilon_g + \frac{L_g}{2}\eta_k^2 \\
&\quad + \frac{8}{3}\eta_k(\alpha_k\sigma_g + c_1\sqrt{\alpha_k}\sigma_g + \frac{9}{4}c_2L_h\frac{\eta_k^2}{\alpha_k^2} + 2c_3L_g\frac{\eta_k^2}{\alpha_k}\bar{\delta}).
\end{aligned} \tag{37}$$

Unrolling this recursion, we have

$$\begin{aligned}
J^\star - \mathbb{E}[J(\theta_K)] &\leq \frac{\eta_0}{3}\epsilon_g + \frac{J^\star - \mathbb{E}[J(\theta_0)]}{(K+1)^2} + c_3\frac{16\eta_0^2}{3}\frac{L_g}{(K+1)^{\frac{7}{5}}}\bar{\delta} + \frac{\eta_0^2}{2}\frac{L_g}{K+1} + \frac{8\eta_0}{3}\frac{\sigma_g}{(K+1)^{\frac{4}{5}}} \\
&\quad + c_1\frac{8\eta_0}{3}\frac{\sigma_g}{(K+1)^{\frac{2}{5}}} + 6c_2\eta_0^3\frac{L_h}{(K+1)^{\frac{2}{5}}}.
\end{aligned} \tag{38}$$

Note that, introduced in Lemma 4.4, the discount factor γ is contained in $L_g = O((1-\gamma)^{-2})$ and $L_h = O((1-\gamma)^{-3})$. Comparing with the definition of ϵ_g in Lemma 4.5, we choose $\eta_0 = \frac{3\mu_F}{M_g}$ for the criteria. Thus, to satisfy $J^\star - \mathbb{E}[J(\theta_K)] \leq \epsilon + \frac{\sqrt{\epsilon_{bias}}}{1-\gamma}$, we have the iteration complexity $K = O(\epsilon^{-2.5})$. In our algorithms, the sample complexity is equal to the iteration complexity, which is also $O(\epsilon^{-2.5})$.

Received 8 April 2024